Lab on a Chip

Cite this: *Lab Chip*, 2012, **12**, 1771

www.rsc.org/loc

TECHNICAL INNOVATION

Scanning laser pulses driven microfluidic peristaltic membrane pump

Yue Chen,*[a] Ting-Hsiang Wu[ab] and Pei-Yu Chiou*[a]

Received 19th January 2012, Accepted 27th February 2012
DOI: 10.1039/c2lc40079k

We reported a pulsed laser driven peristaltic pump for driving fluid in multilayer polydimethylsiloxane (PDMS) microchannels. By synchronizing the dynamics of deforming membrane valves with pulsed laser generated bubbles, a maximum pumping rate of 460 pl s^{-1} has been achieved.

Introduction

Pneumatically controlled PDMS based peristaltic pumps have been widely used in microfluidic devices.[1] Through sequential application of air pressure to close linearly arranged membrane valves, fluid in microchannels can be pumped, guided, and mixed to achieve multistep chemical and biochemical analyses.[2,3] However, interfacing external tubing on a PDMS chip is time consuming, and microfluidic control circuitries become complicated when the number of channels increases. Pneumatic actuation through long tubing also increases the response time of membrane valves.[1] Piezoelectric actuators have been used to actuate a peristaltic pump but its small displacement requires a large-area actuator to provide sufficient actuation volume, which increases the device footprint size.[4] An electrostatic force driven peristaltic pump has also been studied, but the actuation force and the throughput are limited by the small electrostatic energy density.[5,6]

Pulsed laser induced cavitation is a promising mechanism for high speed micro- and nano-fluid actuation. Several microfluidic functions such as high-speed microparticle switching,[7] fluid pumping,[8,9] droplet generation,[10] and cell sorting[11] have been demonstrated with laser-induced cavitations. A tightly focused laser pulse can induce water molecule breakdown and create localized high temperature plasma to instantly vaporize water, and induce rapidly expanding cavitation bubbles. The high vapor pressure inside a laser induced cavitation bubble can provide large mechanical forces to actuate surrounding fluid and structures. Such high-speed and localized fluid flow has been applied for cell lysing,[12] inducing transient cell membrane permeability for gene delivery, and microparticle transport.[13–15] By shaping a laser beam using holography techniques with a spatial light modulator, multiple cavitation bubbles of different shapes can be generated to create desired fluid flows to deform nanostructures such as carbon nanotubes.[16] Laser heating of metal pads integrated on a microfluidic device has also achieved fluid pumping *via* vapor bubbles.[17] By laser heating of metallic nanostructures, patterned nanocavitation can also generate localized high-speed nanofluidic flow to cut fragile mammalian cell membrane for large cargo delivery.[13–15]

Fluid pumping using conventional laser heating induced bubbles, however, has several drawbacks. First, cavitation bubbles triggered by laser-induced breakdown processes usually accompany reactive oxygen species and free-electrons which are toxic to cells and cause biomolecule, such as DNA, damage.[18] Light absorption dyes are also commonly added in the excitation medium to lower the threshold energy of water breakdown.[16] These dyes could also be potential contaminants to the samples under analysis. Second, vapor bubbles induced by continuous wave (CW) laser heating of metal structures could cause potential heating problems to samples close to heated pads.[19]

Here, we demonstrate a new laser-induced cavitation driven peristaltic membrane pump in which cavitation bubbles are induced in a separate channel from the sample channel to completely eliminate any potential contaminants, such as reactive chemicals, dyes, and heat, resulting from the laser cavitation processes. Fluid in the sample channel is driven to move by sequentially deforming thin PDMS membranes between the sample and the laser excitation channels. Compared to conventional pneumatic driven processes, this new light pumping process eliminates the tubing required for fluid control and replaces it with an optical scanner that does not have to physically interface with microfluidic chips.

Fig. 1 shows the schematic of a prototype, three-phase pulsed laser driven peristaltic pump. It is a two-layer PDMS microfluidic device consisting of a bottom folded control channel and a top sample channel. The bottom channel is 75 μm in height, 500 μm in width and the top flow channel is 16 μm in height and 100 μm in width. Fluid in the control and sample channels is separated by 50 μm thick membranes to prevent cross-contamination between channels.

To achieve tight focusing of laser pulses in the control channel under membrane valves separated by mm distances, a linear array of fused silica ball lenses is custom-constructed to focus laser pulses at the middle of the control channel to induce

[a]*Department of Mechanical and Aerospace Engineering, University of California at Los Angeles (UCLA), 43-147 Eng. IV, 420 Westwood Plaza, Los Angeles, CA, 90095-1597, USA. E-mail: pychiou@seas.ucla.edu; katechen@ucla.edu; Fax: +1-310-206-4830; Tel: +1-310-825-8620*
[b]*Department of Pathology and Pediatrics, University of California at Los Angeles (UCLA), Los Angeles, CA, 90095-1732, USA. E-mail: tsw2008@ucla.edu*

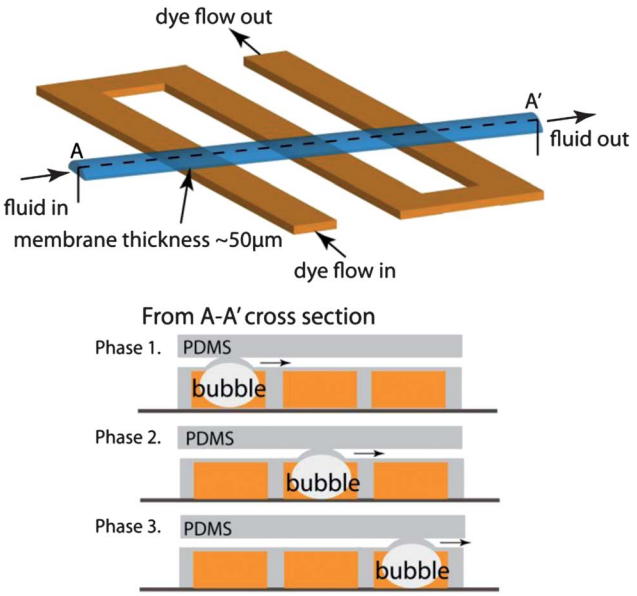

Fig. 1 Schematic of a pulsed laser driven peristaltic membrane pump. The synchronized laser induced cavitation bubbles deform the thin membranes in sequence to push the fluid in the sample channel forward. The laser pulsing channel and the sample delivery channel are separated by a thin membrane valve to eliminate cross-contamination.

cavitation bubbles under these membrane valves. A red color dye (Allura Red AC, Sigma-Aldrich) is added in the control channel to lower the pulse energy threshold. A high repetition rate pulsed laser is used to generate a stream of laser pulses that are scanned and delivered into target channels by an acousto-optic deflector (AOD). The size and lifetime of a laser induced cavitation bubble are pulse energy dependent. The dynamics of induced cavitation bubbles and the deformed PDMS membrane valve are different. It is critical to synchronize the laser pulsing frequency with the membrane deforming dynamics.

The experimental setup is illustrated in Fig. 2(a). A Q-switched Nd:YVO4 pulsed laser (Jazz 20, EKSPLA) is used to excite cavitation bubbles. The laser pulse duration is 8 ns; the wavelength is 532 nm. An AOD (46080-3-LTD, Gooch & Housego) is used to scan these pulses and achieve pulse-on-demand delivery into target channels. Three fused silica ball lenses (Edmund Optics Inc., NJ) 5 mm in diameter are linearly arranged and each separated by a 1 mm gap to focus these pulses into the target locations in the control channel. Fig. 2(b) presents three cavitation bubbles excited by scanning laser pulses of 90 μJ across these ball lenses. A custom-built time-resolved imaging system is used to capture the dynamics of rapidly expanding and collapsing cavitation bubbles and the deformation of membrane valves. A flash lamp (NANOLITE, KL-M, High-Speed Photo-Systems Ltd), synchronized with laser pulses, is used to provide a short exposure time to take the time-resolved images using a CCD camera. A notch filter in front of the camera blocks the high intensity laser pulses during imaging. Since the laser-induced water breakdown process generates hot plasma emitting broadband optical signals,[18] bright spots are captured in the middle of the cavitation bubbles if the CCD camera is exposed for a long time. A Labview FPGA card (PCI-7831R, NI) is used to

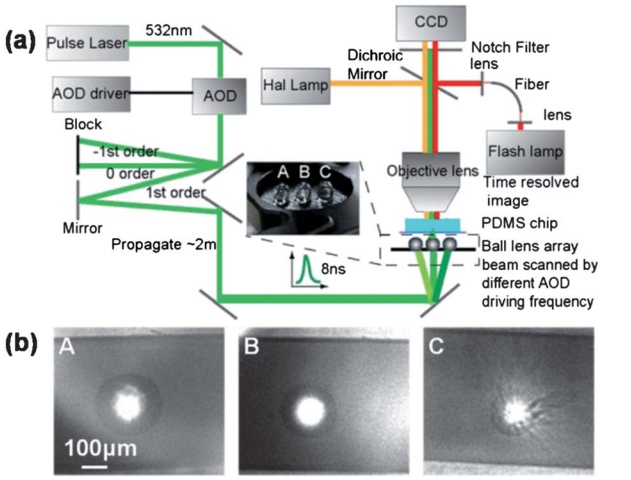

Fig. 2 (a) Experimental setup of the pulsed laser driven peristaltic membrane pump and the time-resolved imaging system. A high repetition rate pulsed laser is scanned by an AOD to deliver laser pulses into target locations through an array of fused silica ball lenses to excite cavitation bubbles as shown in (b). The pulse energy is 90 μJ and the separation distance between bubbles is 6 mm.

synchronize the pulsed laser, AOD scanner, CCD camera, and flash lamp illumination.

Results and discussion

Pulsed laser induced cavitation bubbles can produce large forces and have fast dynamics. An observable bubble can be seen under a microscope in nanoseconds after receiving a laser pulse and rapidly expands to hundreds of micrometres within a microsecond. After expanding to its maximum diameter, the bubble starts to collapse. The lifetime of a bubble is size dependent and ranges from less than a microsecond to longer than a millisecond. Fig. 3 shows a laser cavitation bubble induced by a 108 μJ laser pulse through a 100× objective in the middle of a 50 μm wide PDMS channel filled with DI water. This high pressure bubble quickly expands at a speed higher than 100 m s^{-1} and creates strong mechanical forces on the channel wall. The large bubble forces deform and expand the solid 50 μm wide PDMS channel to more than 100 μm near the excitation site in 273 ns, proving the large force and fast dynamic nature of laser-induced cavitation bubbles and its potential to drive peristaltic pumps in microfluidics.

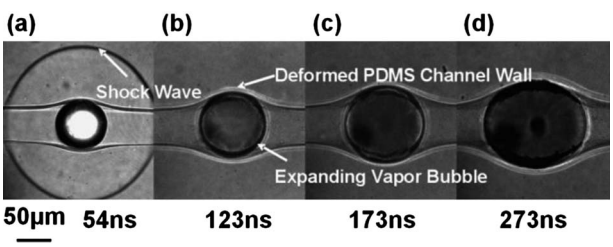

Fig. 3 A 108 μJ laser pulse focused by a 100× objective in the middle of a 50 μm wide channel excites an explosive bubble that quickly expands the channel width to 100 μm. The deformed channel restored to its initial shape 10 μs after excitation in this case.

Fig. 4 shows the deformation of a membrane valve in a multilayer PDMS microfluidic device driven by a cavitation bubble. In this test, the top channel is filled up with air and no fluid. The choice of air instead of fluid is to enhance the optical refractive index contrast for imaging the membrane sealing process under actuation. The bubble reaches its maximum size at 7 μs after the arrival of a laser pulse (Fig. 4(b)). The PDMS membrane is deformed by the expanding bubble to seal the top channel. This bubble fully collapses after 40 μs, but the PDMS membrane valve remains closed (Fig. 4(c)). The membrane restores back to its initial location after 188 μs (Fig. 4(d)).

To test the pumping function, laser pulses with 100 μJ pulse energy are programmed to scan at the three membrane valves in a synchronized sequence. The flow movement is measured on chip by recording the air–liquid interface inside a channel as shown in Fig. 5(a)–(c). The pumping rate is scan frequency dependent (Fig. 5(d)). A maximum pumping rate of 460 pl s^{-1} is observed at 557 Hz (each membrane valve deforms at a repetition rate of 557 cycles per s). Before this liquid–air interface is a 2 cm long microfluidic channel connected to a liquid reservoir through a 30 cm long tubing, proving that the laser scanned peristaltic pump is sufficient to pump liquid across a chip. At the 557 Hz scan frequency, the delay time between neighboring membranes is 600 μs. At higher scanning frequencies, the pumping rates decrease dramatically due to the decrease of the laser pulse energy owing to the slow response of the AOD scanner as shown in Fig. 5(e). Since laser induced breakdown process is a nonlinear optical process, decreasing pulse energy strongly affects the bubble size. The maximum pumping rate occurring at 557 Hz corresponds to the frequency where the energy starts to decay. Pulse energy below the threshold cannot even generate a bubble.

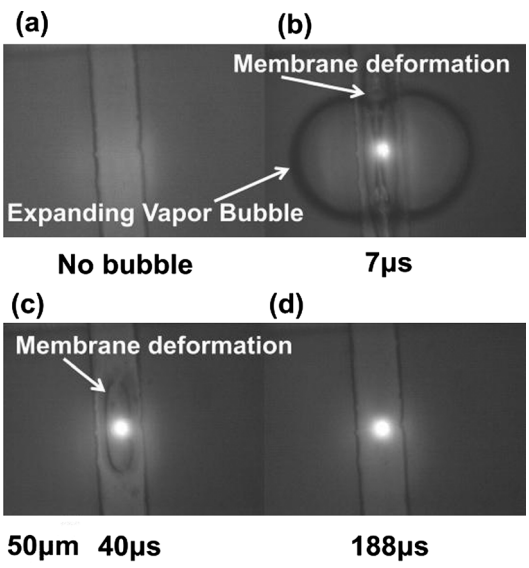

Fig. 4 Time-resolved images showing the fluid–structure interaction between a cavitation bubble and a deformed PDMS channel. (a and b) A bubble excited by a 100 μJ laser pulse in the bottom control channel. The expanding bubble deforms the thin PDMS membrane to close the top channel filled with air. (c) This bubble collapses but the PDMS membrane remains touching the top of the sample channel. (d) After 188 μs, the membrane valve restores to its initial location.

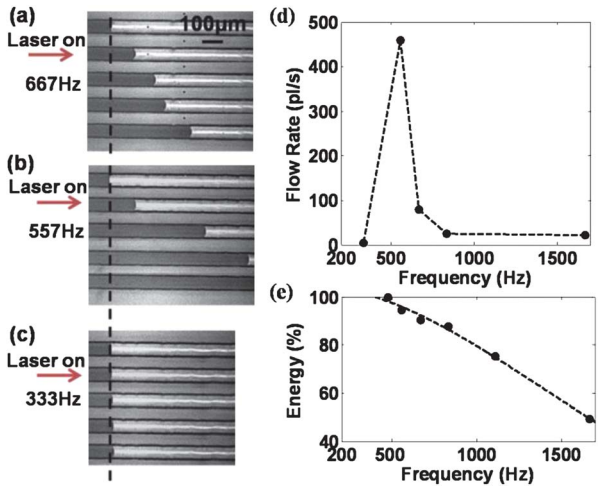

Fig. 5 Pumping rate testing at different scan frequencies. The sample channel is 16 μm in height and 100 μm in width. (a–c) Images captured every 3 s show the moving liquid–air interface. (d) The average flow rate at different frequencies. The observed maximum flow rate is 460 pl s^{-1} at 557 Hz. (e) The decay of pumping rate at higher frequencies is due to the slow AOD scanner, which decreases the pulse energy at high scanning rates.

In our system, the threshold pulse energy is 25 μJ. A high pumping rate can be achieved with a faster scanner since the 600 μs excitation delay time between neighboring membrane valves is much longer than the 188 μs membrane restore time, meaning that part of the fluid pushed by the membrane valve forward is sucked back before the next valve is excited to close the channel, which decreases the efficiency of the peristaltic pump. The effect could further deteriorate at low frequency and is responsible for the low pumping rate when the laser scanning efficiency is lower than 333 Hz, in which case most of the fluid pushed forward by a membrane valve might be completely sucked back before the next neighboring valve is excited.

Conclusions

In sum, we demonstrate a proof-of-concept laser pulses driven peristaltic membrane pump capable of driving fluid flow in a multilayer PDMS microfluidic channel by scanning light pulses. It is realized by utilizing laser-induced cavitation bubbles to sequentially deform linearly arranged membrane valves. The dynamics of the laser induced cavitation bubble and the deformed PDMS membrane have been studied with a time-resolved imaging method. The results show that a laser pulse of 100 μJ energy can excite a cavitation bubble with a maximum size of 370 μm and a lifetime of 40 μs in the control channel. A bubble of this size provides sufficient forces to deform the membrane valve for fluid pumping. By using three linearly arranged membrane valves and sequentially pulsing it, a maximum flow rate of 460 pl s^{-1} has been recorded at a scan frequency of 557 Hz. The pumping rate in our current setup is limited by the speed of the AOD scanner, which lowers the pulse energy at high scanning rates. One major advantage of the laser pulses driven pumping mechanism is the elimination of interconnects required to control

these valves, which simplifies the device structures and fluid control circuitries.

The current device can be further optimized for higher pumping rates either by using a faster scanner to reduce the excitation delay time between two neighboring membrane valves or by fabricating a thinner partition membrane with slower dynamics to match the speed of the current scanner.

Acknowledgements

This project is supported in parts by the NSF grants DBI 0852701, ECCS 0901154, and a UC Discovery/Abraxis BioScience Biotechnology Award #178517.

Notes and references

1 M. A. Unger, H.-P. Chou, T. Thorsen, A. Scherer and S. R. Quake, *Science*, 2000, **288**, 113.
2 H.-P. Chou, M. A. Unger and S. R. Quake, *Biomed. Microdevices*, 2001, **3**(4), 323.
3 O. C. Jeong and S. Konishi, *Sens. Actuators, A*, 2007, **135**, 849.
4 L.-S. Jang and Y.-C. Yu, *Microsyst. Technol.*, 2008, **14**, 241.
5 Q. Lin, B. Yang, J. Xie and Y. C. Tai, *J. Micromech. Microeng.*, 2007, **17**, 220.
6 J. Xie, J. Shih, Q. Lin, B. Yang and Y. C. Tai, *Lab Chip*, 2004, **4**, 495.
7 T.-H. Wu, L. Gao, Y. Chen, K. Wei and P.-Y. Chiou, *Appl. Phys. Lett.*, 2008, **93**, 144102.
8 R. Dijkink and C.-D. Ohl, *Lab Chip*, 2008, **8**, 1676.
9 G. R. Wang, J. G. Santiago, M. G. Mungal, B. Young and S. Papademetriou, *J. Micromech. Microeng.*, 2004, **14**, 1037–1046.
10 S.-Y. Park, T.-H. Wu, Y. Chen, M. A. Teitell and P.-Y. Chiou, *Lab Chip*, 2011, **11**, 1010.
11 T.-H. Wu, Y. Chen, S. Park, J. Hong, T. Teslaa, J. Zhong, D. Di Carlo, M. A. Teitell and P. Y. Chiou, *Lab Chip*, 2012, **12**, 1378–1383.
12 K. R. Rau, P. A. Quinto-Su, A. N. Hellman and V. Venugopalan, *Biophys. J.*, 2006, **91**, 317.
13 C. T. French, I. J. Toesca, T.-H. Wu, T. Teslaa, W. Wong, M. Liu, P.-Y. Chiou, M. A. Teitell and J. F. Miller, *Proc. Natl. Acad. Sci. U. S. A.*, 2011, **108**, 12095.
14 T.-H. Wu, T. Teslaa, S. Kalim, C. T. French, S. Moghadam, R. Wall, J. F. Miller, O. N. Witte, M. A. Teitell and P.-Y. Chiou, *Anal. Chem.*, 2011, **83**, 1321.
15 T.-H. Wu, T. Teslaa, M. A. Teitell and P.-Y. Chiou, *Opt. Express*, 2010, **18**, 23153.
16 P. A. Quinto-Su, X. H. Huang, S. R. Gonzalez-Avila, T. Wu and C. D. Ohl, *Phys. Rev. Lett.*, 2010, **104**, 014501.
17 K. Zhang, A. Jian, X. Zhang, Y. Wang, Z. Li and H.-Y. Tam, *Lab Chip*, 2011, **11**, 1389.
18 A. Vogel, J. Noack, G. Huttman and G. Paltauf, *Appl. Phys. B: Lasers Opt.*, 2005, **81**, 1015–1047.
19 W. T. Nichols, T. Sasaki and N. Koshizaki, *J. Appl. Phys.*, 2006, **100**, 114913.